Steel and Composite Structures, *Vol. 18, No. 1 (2015) 187-212*
DOI: http://dx.doi.org/10.12989/scs.2015.18.1.187

Free vibration analysis of functionally graded plates with temperature-dependent properties using various four variable refined plate theories

Amina Attia [1], Abdelouahed Tounsi [*1,2], E.A. Adda Bedia [1] and S.R. Mahmoud [3,4]

[1] *Material and Hydrology Laboratory, University of Sidi Bel Abbes, Faculty of Technology, Civil Engineering Department, Algeria*
[2] *Advanced Materials and Structures Laboratory, University of Sidi Bel Abbes, Faculty of Technology, Civil Engineering Department, Algeria*
[3] *Department of Mathematics, Faculty of Science, King Abdulaziz University, Saudi Arabia*
[4] *Mathematics Department, Faculty of Science, University of Sohag, Egypt*

(*Received March 23, 2014, Revised April 29, 2014, Accepted May 06, 2014*)

Abstract. In this paper, various four variable refined plate theories are presented to analyze vibration of temperature-dependent functionally graded (FG) plates. By dividing the transverse displacement into bending and shear parts, the number of unknowns and governing equations for the present model is reduced, significantly facilitating engineering analysis. These theories account for parabolic, sinusoidal, hyperbolic, and exponential distributions of the transverse shear strains and satisfy the zero traction boundary conditions on the surfaces of the plate without using shear correction factors. Power law material properties and linear steady-state thermal loads are assumed to be graded along the thickness. Uniform, linear, nonlinear and sinusoidal thermal conditions are imposed at the upper and lower surface for simply supported FG plates. Equations of motion are derived from Hamilton's principle. Analytical solutions for the free vibration analysis are obtained based on Fourier series that satisfy the boundary conditions (Navier's method). Non-dimensional results are compared for temperature-dependent and temperature-independent FG plates and validated with known results in the literature. Numerical investigation is conducted to show the effect of material composition, plate geometry, and temperature fields on the vibration characteristics. It can be concluded that the present theories are not only accurate but also simple in predicting the free vibration responses of temperature-dependent FG plates.

Keywords: functionally graded plate; higher-order plate theory; vibration; temperature-dependent properties

1. Introduction

Functionally graded materials (FGMs) are a class of composites that have continuous variation of material properties from one surface to another and thus eliminate the stress concentration

∗Corresponding author, Professor, E-mail: tou_abdel@yahoo.com

http://www.techno-press.org/?journal=scs&subpage=8 ISSN: 1229-9367 (Print), 1598-6233 (Online)

found in laminated composites. The concept of FGM has been widely explored in various engineering applications including mechanical, aerospace, nuclear, and civil engineering. The increase in FGM applications requires accurate models to predict their responses. Since the shear deformation has significant effects on the responses of functionally graded (FG) plates, shear deformation theories are used to capture such shear deformation effects. The first-order shear deformation theory (Mindlin 1951, Reissner 1945) accounts for shear deformation effects, but violates the equilibrium conditions at the top and bottom surfaces of the plate. A shear correction factor is therefore required (Yaghoobi and Yaghoobi 2013). The higher-order shear deformation theories (Reddy 1984, 2000, Ren 1986, Touratier 1991, Soldatos 1992, Xiang *et al*. 2009, Akavci 2010, Grover *et al*. 2013, Karama *et al*. 2003, Pradyumna and Bandyopadhyay 2008, Ait Atmane *et al*. 2010, Shahrjerdi *et al*. 2011, Mantari *et al*. 2012) account for higher-order variation in the in-plane displacements through the thickness of the plate and satisfy the equilibrium conditions at the top and bottom surfaces of the plate without requiring any shear correction factors. Some of these HSDTs are computational costs because with each additional power of the thickness coordinate, an additional unknown is introduced to the theory. Although some well-known higher-order shear deformation theories have the same unknowns as in the first-order shear deformation theory (e.g., third-order shear deformation theory (Reddy 1984 and 2000), sinusoidal shear deformation theory (Touratier 1991), hyperbolic shear deformation theory (Xiang *et al*. 2009, Akavci 2010, Grover *et al*. 2013), exponential shear deformation theory (Karama *et al*. 2003), second-order shear deformation theory (Shahrjerdi *et al*. 2011), and trigonometric shear deformation theory (Mantari *et al*. 2012)), their equations of motion are more complicated than those of the first-order shear deformation theory. Recently, new refined plate theories for bending response, buckling and free vibration of FG plates with only four unknown functions are developed (Bourada *et al*. 2012, Fekrar *et al*. 2012, Bouderba *et al*. 2013, Kettaf *et al*. 2013, Ait Atmane Meziane *et al*. 2014). However, many of the above-mentioned papers deal with temperature-independent materials with shear deformation theories. Temperature-dependent materials in a constant temperature field and temperature variations with surface-to-surface heat flow through the thickness direction were considered in other research by applying first, third and higher order shear deformation theories. As a consequence, the development of simple higher-order shear deformation theory for temperature-dependent FG plates in the present work is necessary.

The aim of this work is to develop a simple higher-order shear deformation theory for free vibration behavior of temperature-dependent FG plates. The proposed theory contains fewer unknowns and equations of motion than the first-order shear deformation theory, but satisfies the equilibrium conditions at the top and bottom surfaces of the plate without using any shear correction factors. The displacement fields of the proposed theories are chosen based on cubic, sinusoidal, hyperbolic, and exponential variation in the in-plane displacements through the thickness. Partitioning the transverse displacement into the bending and shear components leads to a reduction in the number of unknowns, and consequently, makes the present theory much more amenable to mathematical implementation. The temperature is assumed to be constant in the plane of the plate. The variation of temperature is assumed to occur in the thickness direction only. The FG plates are assumed to be simply supported with temperature-dependent and independent material properties with a power law distribution in terms of the volume fractions of the constituents and subjected to uniform, linear, nonlinear and sinusoidal temperature rise. Equations of motion are derived from Hamilton's principle. The effects of temperature dependency of FG plates for some types of thermal condition are investigated. The current study is relevant to aero-structures.

2. Theoretical developments

Consider a simply supported rectangular FG plate with the length a width b, and thickness h. The x-, y-, and z-coordinates are taken along the length, width, and height of the plate, respectively, as shown in Fig. 1. The formulation is limited to linear elastic material behavior. The FG plate is isotropic with its material properties vary smoothly through the thickness of the plate.

2.1 Displacement field and strains

The formulation is limited to linear elastic material behavior. The displacement fields of various shear deformation theories are chosen based on following assumptions: (1) The transverse displacement is partitioned into bending and shear components; (2) the in-plane displacements are partitioned into extension, bending and shear components; (3) the bending parts of the in-plane displacements are similar to those given by the classical plate theory (CPT); and (4) the shear component of axial displacement gives rise to the higher-order variation of shear strain and hence to shear stress through the thickness of the plate in such a way that shear stress vanishes on the top and bottom surfaces. Based on these assumptions, the displacement fields of various higher-order shear deformation theories are given in a general form as

$$\begin{aligned} u(x,y,z,t) &= u_0(x,y,t) - z\frac{\partial w_b}{\partial x} - f(z)\frac{\partial w_s}{\partial x} \\ v(x,y,z,t) &= v_0(x,y,t) - z\frac{\partial w_b}{\partial y} - f(z)\frac{\partial w_s}{\partial y} \\ w(x,y,z,t) &= w_b(x,y,t) + w_s(x,y,t) \end{aligned} \tag{1}$$

where u_0 and v_0 denote the displacements along the x and y coordinate directions of a point on the mid-plane of the plate; w_b and w_s are the bending and shear components of the transverse displacement, respectively. $f(z)$ is a shape function determining the distribution of the transverse shear strain and shear stress through the thickness of the plate given in Table 1. The shape functions $f(z)$ are chosen to satisfy the stress-free boundary conditions on the top and bottom

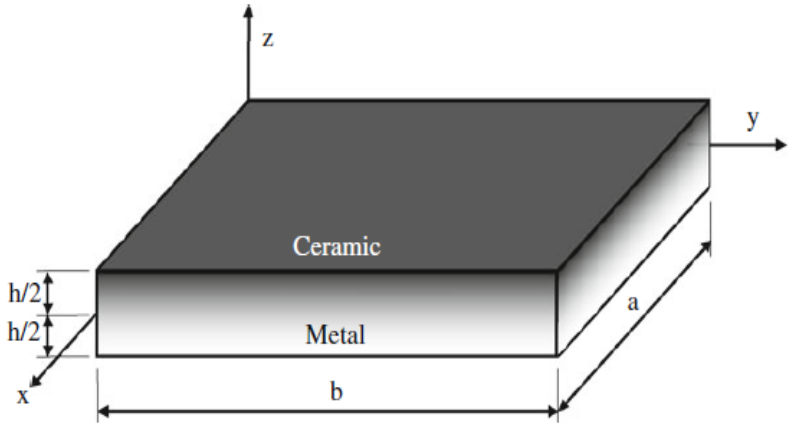

Fig. 1 Schematic representation of a rectangular FG plate

Table 1 Shape functions

model	$f(z)$	$g(z) = 1 - f'(z)$
Third plate theory (TPT)	$\frac{4z^3}{3h^2}$	$1-\frac{4z^2}{h^2}$
Sinusoidal plate theory (SPT)	$z-\frac{h}{\pi}\sin\left(\frac{\pi z}{h}\right)$	$\cos\left(\frac{\pi z}{h}\right)$
Hyperbolic plate theory (HPT)	$z-h\sinh\left(\frac{z}{h}\right)+z\cosh\frac{1}{2}$	$\cosh\left(\frac{z}{h}\right)-\cosh\frac{1}{2}$
Exponential plate theory (EPT)	$z-ze^{-2(z/h)^2}$	$\left(1-\frac{4z^2}{h^2}\right)e^{-2(z/h)^2}$

surfaces of the plate, thus a shear correction factor is not required.

The nonzero linear strains associated with the displacement field in Eq. (2) are

$$\begin{Bmatrix}\varepsilon_x\\ \varepsilon_y\\ \gamma_{xy}\end{Bmatrix}=\begin{Bmatrix}\varepsilon_x^0\\ \varepsilon_y^0\\ \gamma_{xy}^0\end{Bmatrix}+z\begin{Bmatrix}k_x^b\\ k_y^b\\ k_{xy}^b\end{Bmatrix}+f(z)\begin{Bmatrix}k_x^s\\ k_y^s\\ k_{xy}^s\end{Bmatrix},\quad \begin{Bmatrix}\gamma_{yz}\\ \gamma_{xz}\end{Bmatrix}=g(z)\begin{Bmatrix}\gamma_{yz}^0\\ \gamma_{xz}^0\end{Bmatrix}, \tag{2}$$

where

$$\begin{Bmatrix}\varepsilon_x^0\\ \varepsilon_y^0\\ \gamma_{xy}^0\end{Bmatrix}=\begin{Bmatrix}\frac{\partial u_0}{\partial x}\\ \frac{\partial v_0}{\partial x}\\ \frac{\partial u_0}{\partial y}+\frac{\partial v_0}{\partial x}\end{Bmatrix},\begin{Bmatrix}k_x^b\\ k_y^b\\ k_{xy}^b\end{Bmatrix}=\begin{Bmatrix}-\frac{\partial^2 w_b}{\partial x^2}\\ -\frac{\partial^2 w_b}{\partial y^2}\\ -2\frac{\partial^2 w_b}{\partial x\partial y}\end{Bmatrix},\begin{Bmatrix}k_x^s\\ k_y^s\\ k_{xy}^s\end{Bmatrix}=\begin{Bmatrix}-\frac{\partial^2 w_s}{\partial x^2}\\ -\frac{\partial^2 w_s}{\partial y^2}\\ -2\frac{\partial^2 w_s}{\partial x\partial y}\end{Bmatrix},\begin{Bmatrix}\gamma_{yz}^0\\ \gamma_{xz}^0\end{Bmatrix}=\begin{Bmatrix}\frac{\partial w_s}{\partial y}\\ \frac{\partial w_s}{\partial x}\end{Bmatrix}, \tag{3}$$

and

$$g(z)=1-f'(z) \tag{4}$$

2.2 Constitutive relations

FGMs are composite materials made of ceramic and metal. There are some models in the literature that express the variation of material properties in FGMs (Chi and Chung 2006a, b).The most commonly used is the power law distribution of the volume fraction. According to this model, the material properties of FG plates are assumed to be position and temperature- dependent and can be expressed as the following (Kim 2005)

$$\Gamma(z,T)=\left(\Gamma_c(T)-\Gamma_m(T)\right)V_c+\Gamma_m(T)\quad\text{and}\quad V_c(z)=\left(\frac{z}{h}+\frac{1}{2}\right)^p \tag{5}$$

where Γ denotes a generic material property such as elastic modulus E, the Poisson's ratio v, mass

density ρ and thermal expansion coefficient α of FG plates; furthermore subscripts m and c refer to the pure metal and ceramic plates, respectively. V_c denotes the ceramic volume fraction, where $p \geq 0$ is a namely grading index that is the volume fraction exponent. The non-linear FG plate's material can be expressed as the following (Shahrjerdi *et al*. 2011)

$$P(T) = P_0\left(P_{-1}T^{-1} + 1 + P_1T + P_2T^2 + P_3T^3\right) \tag{6}$$

where P denotes material property and $T = T_0 + \Delta T(z)$ indicates the environmental temperature; $T_0 = 300(K)$ is room temperature; P_{-1}, P_0, P_1, P_2 and P_3 are the coefficients of temperature-dependent material properties unique to the constituent materials, and $\Delta T(z)$ is the temperature rise only through the thickness direction, whereas thermal conductivity k is temperature-independent. Temperature-dependent typical values for some functionally graded materials components such as silicon nitride and stainless steel are in Table 2 (Shahrjerdi *et al*. 2011, Kim 2005).

The linear constitutive relations of a FG plate can be written as

$$\begin{Bmatrix} \sigma_x \\ \sigma_y \\ \tau_{yz} \\ \tau_{xz} \\ \tau_{xy} \end{Bmatrix} = \begin{bmatrix} C_{11} & C_{12} & 0 & 0 & 0 \\ C_{12} & C_{22} & 0 & 0 & 0 \\ 0 & 0 & C_{44} & 0 & 0 \\ 0 & 0 & 0 & C_{55} & 0 \\ 0 & 0 & 0 & 0 & C_{66} \end{bmatrix} \begin{Bmatrix} \varepsilon_x \\ \varepsilon_y \\ \gamma_{yz} \\ \gamma_{xz} \\ \gamma_{xy} \end{Bmatrix} \tag{7}$$

where (σ_x, σ_y, τ_{yz}, τ_{xz}, τ_{xy}) and (ε_x, ε_y, γ_{yz}, γ_{xz}, γ_{xy}) are the stress and strain components, respectively. Using the material properties defined in Eq. (5), stiffness coefficients, C_{ij}, can be expressed as

$$C_{11} = C_{22} = \frac{E(z,T)}{1-\nu^2(z,T)}, \tag{8a}$$

$$C_{12} = \nu(z,T)C_{11}, \tag{8b}$$

$$C_{44} = C_{55} = C_{66} = \frac{E(z,T)}{2\left(1+\nu(z,T)\right)}, \tag{8c}$$

2.3 Equations of motion

The total strain energy of FG plate is given by

$$U = U_p + U_T \tag{9}$$

where U_p and U_T are the strain energies due to mechanical and thermal effects, respectively.

The strain energies U_p and U_T are given by (Shahrjerdi *et al*. 2011, Li *et al*. 2009, Reddy 2004)

$$U_p = \frac{1}{2}\int_V \left[\sigma_x\,\varepsilon_x + \sigma_y\,\varepsilon_y + \tau_{xy}\,\gamma_{xy} + \tau_{yz}\,\gamma_{yz} + \tau_{xz}\,\gamma_{xz}\right]dV \tag{10a}$$

$$U_T = \frac{1}{2}\int_V \left[\sigma_x^T d_{11} + \sigma_y^T d_{22}\right]dV \tag{10b}$$

Table 2 Temperature-dependent coefficients for ZrO_2/Ti-6Al-4V and SI_3N_4/SUS304

Material		P_{-1}	P_0	P_1	P_2	P_3
E	SUS304	0	201.04e^{+9}	3.079e^{-3}	-6.534e^{-7}	0
	SI_3N_4	0	348.43e^{+9}	-3.070e^{-4}	2.160e^{-7}	-8.946e^{-11}
	Ti-6Al-4V	0	122.56e^{+9}	-4.586e^{-4}	0	0
	ZrO_2	0	244.27e^{+9}	-1.371e^{-3}	1.214e^{-6}	-3.681e^{-10}
V	SUS304	0	0.3262	-2.002e^{-4}	3.797e^{-7}	0
	SI_3N_4	0	0.2400	0	0	0
	Ti-6Al-4V	0	0.2888	1.108e^{-4}	0	0
	ZrO_2	0	0.3330	0	0	0
ρ	SUS304	0	8166	0	0	0
	SI_3N_4	0	2370	0	0	0
	Ti-6Al-4V	0	4429	0	0	0
	ZrO_2	0	3000	0	0	0
α	SUS304	0	12.330e^{-6}	8.086e^{-6}	0	0
	SI_3N_4	0	5.8723e^{-6}	9.095e^{-6}	0	0
	Ti-6Al-4V	0	7.5788e^{-6}	6.638e^{-4}	-3.147e^{-6}	0
	ZrO_2	0	12.766e^{-6}	-1.491e^{-3}	1.006e^{-5}	-6.778e^{-11}
k	SUS304	0	12.04	0	0	0
	SI_3N_4	0	9.19	0	0	0
	Ti-6Al-4V	0	7.82	0	0	0
	ZrO_2	0	1.80	0	0	0

where d_{ij}, (i, j = 1, 2) is the nonlinear strain-displacement relationship (Shahrjerdi *et al*. 2011, Reddy 2004). By substituting d_{ij} into Eq. (10b) the following equation is obtained

$$U_T = \frac{1}{2}\int_V \left\{ \sigma_x^T \left[\left(\frac{\partial u}{\partial x}\right)^2 + \left(\frac{\partial v}{\partial x}\right)^2 + \left(\frac{\partial w}{\partial x}\right)^2 \right] + \sigma_y^T \left[\left(\frac{\partial u}{\partial y}\right)^2 + \left(\frac{\partial v}{\partial y}\right)^2 + \left(\frac{\partial w}{\partial y}\right)^2 \right] \right\} dV \tag{10c}$$

with

$$\sigma_x^T = -(C_{11} + C_{12})\alpha(z,T)\Delta T(z) \quad \text{and} \quad \sigma_y^T = -(C_{22} + C_{12})\alpha(z,T)\Delta T(z) \tag{10d}$$

The kinetic energy of plate is given by

$$K = \frac{1}{2}\int_V \rho(z,T)\left[\dot{u} + \dot{v} + \dot{w}\right] dV \tag{11}$$

Hamilton's principle for an elastic body can be represented as

$$\int_{t_1}^{t_2} (\delta U - \delta K) dt = 0 \tag{12}$$

By substituting Eq. (2) into Eq. (7) and applying Eqs. (12) and (1), equations of motion for FG plate can be obtained as follows

$$\begin{aligned}
&\left(A_{11}+A_{11}^{T}\right)d_{11}u_0+\left(A_{66}+A_{22}^{T}\right)d_{22}u_0+\left(A_{12}+A_{66}\right)d_{12}v_0\\
&-\left(B_{11}+B_{11}^{T}\right)d_{111}w_b-(B_{11}^{s}+B_{11}^{sT})d_{111}w_s\\
&-\left(B_{12}+2B_{66}+B_{22}^{T}\right)d_{122}w_b-\left(B_{12}^{s}+2B_{66}^{s}+B_{22}^{sT}\right)d_{122}w_s\\
&=I_0\ddot{u}_0-I_1d_1\ddot{w}_b-J_1d_1\ddot{w}_s,
\end{aligned}\tag{13a}$$

$$\begin{aligned}
&\left(A_{22}+A_{22}^{T}\right)d_{22}v_0+\left(A_{66}+A_{11}^{T}\right)d_{11}v_0+\left(A_{12}+A_{66}\right)d_{12}u_0\\
&-(B_{22}+B_{22}^{T})d_{222}w_b-\left(B_{22}^{s}+B_{22}^{sT}\right)d_{222}w_s\\
&-\left(B_{12}+2B_{66}+B_{11}^{T}\right)d_{112}w_b-\left(B_{12}^{s}+2B_{66}^{s}+B_{11}^{sT}\right)d_{112}w_s\\
&=I_0\ddot{v}_0-I_1d_2\ddot{w}_b-J_1d_2\ddot{w}_s,
\end{aligned}\tag{13b}$$

$$\begin{aligned}
&\left(B_{11}+B_{11}^{T}\right)d_{111}u_0+\left(B_{12}+2B_{66}+B_{22}^{T}\right)d_{122}u_0+\left(B_{12}+2B_{66}+B_{11}^{T}\right)d_{112}v_0+\left(B_{22}+B_{22}^{T}\right)d_{222}v_0\\
&-\left(D_{11}+D_{11}^{T}\right)d_{1111}w_b-\left(D_{11}^{sT}+D_{11}^{s}\right)d_{1111}w_s-2\left(2D_{66}+D_{12}\right)d_{1122}w_b-2\left(D_{12}^{s}+2D_{66}^{s}\right)d_{1122}w_s\\
&-\left(D_{22}+D_{22}^{T}\right)d_{2222}w_b-\left(D_{22}^{s}+D_{22}^{sT}\right)d_{2222}w_s+A_{11}^{T}\left(d_{11}w_s+d_{11}w_b\right)+A_{22}^{T}\left(d_{22}w_b+d_{22}w_s\right)\\
&-\left(D_{11}^{sT}+D_{22}^{sT}\right)d_{1122}w_s-\left(D_{11}^{T}+D_{22}^{T}\right)d_{1122}w_b\\
&=I_0\left(\ddot{w}_b+\ddot{w}_s\right)+I_1\left(d_1\ddot{u}_0+d_2\ddot{v}_0\right)-I_2\left(d_{11}\ddot{w}_b+d_{22}\ddot{w}_b\right)-J_2\left(d_{11}\ddot{w}_s+d_{22}\ddot{w}_s\right)
\end{aligned}\tag{13c}$$

$$\begin{aligned}
&\left(B_{11}^{s}+B_{11}^{s}\right)d_{111}u_0+\left(B_{12}^{s}+2B_{66}^{s}+B_{22}^{sT}\right)d_{122}u_0+\left(B_{12}^{s}+2B_{66}^{s}+B_{11}^{sT}\right)d_{112}v_0+\left(B_{22}^{s}+B_{22}^{sT}\right)d_{222}v_0\\
&-\left(D_{11}^{s}+D_{11}^{sT}\right)d_{1111}w_b-\left(H_{11}^{s}+H_{11}^{sT}\right)d_{1111}w_s-2\left(2D_{66}^{s}+D_{12}^{s}\right)d_{1122}w_b-\left(D_{22}^{s}+D_{22}^{sT}\right)d_{2222}w_b\ -\\
&2\left(H_{12}^{s}+2H_{66}^{s}\right)d_{1122}w_s-(H_{22}^{s}+H_{22}^{sT})d_{2222}w_s+A_{44}^{s}d_{22}w_s+A_{55}^{s}d_{11}w_s+A_{11}^{T}\left(d_{11}w_s+d_{11}w_b\right)+\\
&A_{22}^{T}\left(d_{22}w_b+d_{22}w_s\right)-\left(D_{11}^{sT}+D_{22}^{sT}\right)d_{1122}w_b-\left(H_{11}^{sT}+H_{22}^{sT}\right)d_{1122}w_s\\
&=I_0\left(\ddot{w}_b+\ddot{w}_s\right)+J_1\left(d_1\ddot{u}_0+d_2\ddot{v}_0\right)\\
&=I_0\left(\ddot{w}_b+\ddot{w}_s\right)+J_1\left(d_1\ddot{u}_0+d_2\ddot{v}_0\right)-J_2\left(d_{11}\ddot{w}_b+d_{22}\ddot{w}_b\right)-K_2\left(d_{11}\ddot{w}_s+d_{22}\ddot{w}_s\right)
\end{aligned}\tag{13d}$$

where d_{ij}, d_{ijl} and d_{ijlm} are the following differential operatorsd

$$d_{ij}=\frac{\partial^2}{\partial x_i\partial x_j},\quad d_{ijl}=\frac{\partial^3}{\partial x_i\partial x_j\partial x_l},\quad d_{ijlm}=\frac{\partial^4}{\partial x_i\partial x_j\partial x_l\partial x_m},\quad d_i=\frac{\partial}{\partial x_i},\qquad (i,j,l,m=1,2).\tag{14}$$

and stiffness components are given as

$$\begin{Bmatrix} A_{11} & B_{11} & D_{11} & B_{11}^{s} & D_{11}^{s} & H_{11}^{s}\\ A_{12} & B_{12} & D_{12} & B_{12}^{s} & D_{12}^{s} & H_{12}^{s}\\ A_{66} & B_{66} & D_{66} & B_{66}^{s} & D_{66}^{s} & H_{66}^{s}\end{Bmatrix}=\int_{-h/2}^{h/2}C_{11}\left(1,z,z^2,f(z),z\,f(z),f^2(z)\right)\begin{Bmatrix}1\\ \nu\\ \dfrac{1-\nu}{2}\end{Bmatrix}dz,\tag{15a}$$

$$\left(A_{22}, B_{22}, D_{22}, B_{22}^s, D_{22}^s, H_{22}^s\right) = \left(A_{11}, B_{11}, D_{11}, B_{11}^s, D_{11}^s, H_{11}^s\right), \tag{15b}$$

$$A_{44}^s = A_{55}^s = \int_{-h/2}^{h/2} C_{44}\left[g(z)\right]^2 dz, \tag{15c}$$

$$\begin{Bmatrix} A_{11}^T & B_{11}^T & D_{11}^T & B_{11}^{sT} & D_{11}^{sT} & H_{11}^{sT} \\ A_{22}^T & B_{22}^T & D_{22}^T & B_{22}^{sT} & D_{22}^{sT} & H_{22}^{sT} \end{Bmatrix} = \int_{-h/2}^{h/2} \left(1, z, z^2, f(z), zf(z), f(z)^2\right) \begin{Bmatrix} \sigma_x^T \\ \sigma_y^T \end{Bmatrix} dz \tag{15d}$$

The inertias are also defined as

$$\left(I_0, I_1, J_1, I_2, J_2, K_2\right) = \int_{-h/2}^{h/2} \left(1, z, f, z^2, z\, f, f^2\right) \rho(z) dz \tag{15e}$$

2.4 Temperature field

In this study, four cases of one-dimensional temperature distribution through the thickness are considered, with $T = T(z)$.

2.4.1 Uniform temperature

In this case, a uniform temperature field is used as followsd

$$T(z) = T_0 + \Delta T(z) \tag{16}$$

where $\Delta T(z)$ denotes the temperature change and $T_0 = 300\ K$ is room temperature.

2.4.2 Linear temperature

Assuming temperatures T_b and T_t are imposed at the bottom and top of the plate, the temperature field under linear temperature rise along the thickness can be obtained as

$$T(z) = T_0 + \Delta T\left(\frac{z}{h} + \frac{1}{2}\right) \tag{17}$$

where $\Delta T = T_t - T_b$ is the temperature gradient and $T_0 = 300\ K$ is room temperature.

2.4.3 Nonlinear temperature

The nonlinear temperature rise across the thickness of the plate is determined by solving the one dimensional heat conduction equation. The one dimensional steady-state heat conduction equation in the z-direction is given by

$$-\frac{d}{dz}\left(k(z)\frac{dT}{dz}\right) = 0 \tag{18}$$

with the boundary condition $T(h/2) = T_t$ and $T(-h/2) = T_b = T_0$. Here a stress-free state is assumed

to exist at T_0 = 300 K. The thermal conductivity coefficient $k(z)$ is assumed here to obey the power-law relation in Eq. (5). The analytical solution to Eq. (18) is

$$T(z) = T_b - (T_t - T_b)\frac{\int_{-h/2}^{z} \frac{1}{k(z)} dz}{\int_{-h/2}^{h/2} \frac{1}{k(z)} dz} \tag{19}$$

In the case of power-law FG plate, the solution of Eq. (18) also can be expressed by means of a polynomial series (Shahrjerdi *et al*. 2011)

$$T(z) = T_b + \frac{(T_t - T_b)}{C_{tb}}\left[\left(\frac{2z+h}{2h}\right) - \frac{k_{tb}}{(p+1)k_b}\left(\frac{2z+h}{2h}\right)^{p+1} + \frac{k_{tb}^2}{(2p+1)k_b^2}\left(\frac{2z+h}{2h}\right)^{2p+1}\right.$$
$$\left. - \frac{k_{tb}^3}{(3p+1)k_b^3}\left(\frac{2z+h}{2h}\right)^{3p+1} + \frac{k_{tb}^4}{(4p+1)k_b^4}\left(\frac{2z+h}{2h}\right)^{4p+1} - \frac{k_{tb}^5}{(5p+1)k_b^5}\left(\frac{2z+h}{2h}\right)^{5p+1}\right] \tag{20}$$

with

$$C_{tb} = 1 - \frac{k_{tb}}{(p+1)k_b} + \frac{k_{tb}^2}{(2p+1)k_b^2} - \frac{k_{tb}^3}{(3p+1)k_b^3} + \frac{k_{tb}^4}{(4p+1)k_b^4} - \frac{k_{tb}^5}{(5p+1)k_b^5} \tag{21}$$

where $k_{tb} = k_t - k_b$, with k_t and k_b are the thermal conductivity of the top and bottom faces of the plate, respectively.

2.4.4 Sinusoidal temperature rise

The temperature field under sinusoidal temperature rise across the thickness is assumed as (Shahrjerdi *et al*. 2011, Bouazza *et al*. 2009)

$$T(z) = (T_t - T_b)\left[1 - \cos\left(\frac{\pi z}{2h} + \frac{\pi}{4}\right)\right] + T_b \tag{22}$$

3. Analytical solutions

Based on the Navier approach with simply supported boundary conditions, the displacement fields are expressed as

$$\begin{Bmatrix} u_0 \\ v_0 \\ w_b \\ w_s \end{Bmatrix} = \sum_{m=1}^{\infty}\sum_{n=1}^{\infty} \begin{Bmatrix} U_{mn} e^{i\omega t} \cos(\lambda x)\sin(\mu y) \\ V_{mn} e^{i\omega t} \sin(\lambda x)\cos(\mu y) \\ W_{bmn} e^{i\omega t} \sin(\lambda x)\sin(\mu y) \\ W_{smn} e^{i\omega t} \sin(\lambda x)\sin(\mu y) \end{Bmatrix} \tag{23}$$

where U_{mn}, V_{mn}, W_{bmn} and W_{smn} are arbitrary parameters to be determined, ω is the eigen frequency associated with (m, n) the eigen mode, and $\lambda = m\pi / a$ and $\mu = n\pi / b$.

Substituting the displacement fields (23) into equations of motion (13), the following frequency equation is obtained

$$\left(\begin{bmatrix} a_{11} & a_{12} & a_{13} & a_{14} \\ a_{12} & a_{22} & a_{23} & a_{24} \\ a_{13} & a_{23} & a_{33} & a_{34} \\ a_{14} & a_{24} & a_{34} & a_{44} \end{bmatrix} - \omega^2 \begin{bmatrix} m_{11} & 0 & m_{13} & m_{14} \\ 0 & m_{22} & m_{23} & m_{24} \\ m_{13} & m_{23} & m_{33} & m_{34} \\ m_{14} & m_{24} & m_{34} & m_{44} \end{bmatrix}\right) = \begin{Bmatrix} 0 \\ 0 \\ 0 \\ 0 \end{Bmatrix} \tag{24}$$

in which

$$\begin{aligned}
a_{11} &= -\lambda^2\left(A_{11}+A_{11}^T\right)-\mu^2\left(A_{66}+A_{22}^T\right)\\
a_{12} &= -\lambda\mu\left(A_{12}+A_{66}\right)\\
a_{13} &= \lambda\left[\lambda^2(B_{11}+B_{11}^T)+\left(B_{12}+2B_{66}+B_{22}^T\right)\mu^2\right]\\
a_{14} &= \lambda\left[B_{11}^s\lambda^2+B_{11}^{aT}+\left(B_{12}^s+2B_{66}^s+B_{22}^{sT}\right)\mu^2\right]\\
a_{22} &= -\lambda^2\left(A_{66}+A_{11}^T\right)-\mu^2\left(A_{22}+A_{22}^T\right)\\
a_{23} &= \mu\left[\mu^2(B_{22}+B_{22}^T)+\left(B_{12}+2B_{66}+B_{11}^T\right)\lambda^2\right]\\
a_{24} &= \mu\left[\mu^2(B_{22}^s+B_{22}^{sT})+\left(B_{12}^s+2B_{66}^s+B_{11}^{sT}\right)\lambda^2\right]\\
a_{33} &= -\left[\left(D_{11}+D_{11}^T\right)\lambda^4+D_{22}^T\mu^4+2\left(D_{12}+2D_{66}+D_{22}^T+D_{11}^T\right)\lambda^2\mu^2+D_{22}\mu^4+A_{11}^T\lambda^2+A_{22}^T\mu^2\right]\\
a_{34} &= -\left[\left(D_{11}^s+D_{11}^{sT}\right)\lambda^4+2\left(D_{12}^s+2D_{66}^s+D_{11}^{sT}+D_{22}^{sT}\right)\lambda^2\mu^2+\left(D_{22}^s+D_{22}^{sT}\right)\mu^4+A_{11}^T\lambda^2+A_{22}^T\mu^2\right]\\
a_{44} &= -\left[\left(H_{11}^s+H_{11}^{sT}\right)\lambda^4+\left(H_{22}^{sT}+H_{11}^{sT}+2\left(H_{12}^s+2H_{66}^s\right)\right)\lambda^2\mu^2+\left(H_{22}^s+H_{22}^{sT}\right)\mu^4\right.\\
&\quad \left.+\lambda^2\left(A_{55}^s+A_{11}^T\right)+\mu^2\left(A_{44}^s+A_{22}^T\right)\right]
\end{aligned} \tag{25}$$

$$\begin{aligned}
m_{11} &= I_1\\
m_{12} &= 0\\
m_{13} &= -I_2\lambda\\
m_{14} &= -I_4\lambda\\
m_{22} &= I_1\\
m_{23} &= -I_2\mu\\
m_{24} &= -I_4\mu\\
m_{33} &= I_1+I_3\left(\mu^2+\lambda^2\right)\\
m_{34} &= I_1+I_5\left(\mu^2+\lambda^2\right)\\
m_{44} &= I_1+I_6\left(\mu^2+\lambda^2\right)
\end{aligned}$$

4. Numerical results

4.1 Material properties in thermal conditions

In Figs. 2 to 6, the variation of Young modulus in FG plates through the thickness in room temperature is presented by considering, uniform, linear, nonlinear and sinusoidal thermal

conditions, respectively. Room temperature is defined at $T_0 = 300\ K$ for all thermal conditions. The temperature rise in linear temperature is $T_b = T_t = 600\ (K)$, the nonlinear thermal conditions are $T_b = 0\ (K)$ and $T_t = 600\ (K)$ and the sinusoidal thermal conditions are $T_b = 300\ (K)$ and $T_t = 300\ (K)$.

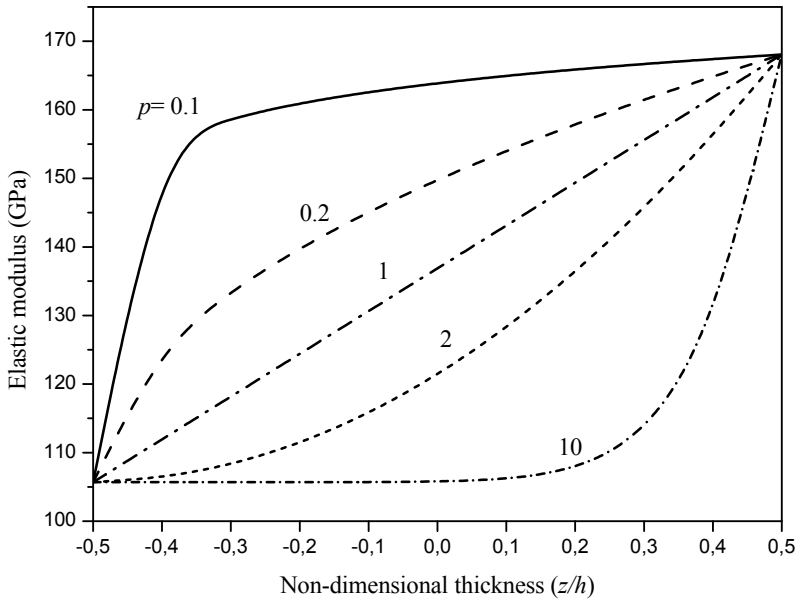

Fig. 2 Variation of elastic modulus versus non-dimensional thickness of FG plate in room temperature field and different values of grading index (p)

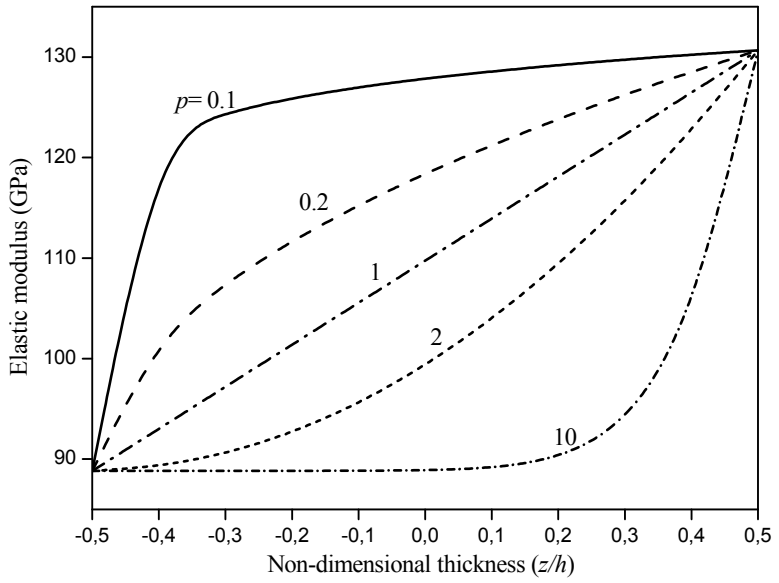

Fig. 3 Variation of elastic modulus versus non-dimensional thickness of FG plate in linear temperature field and different values of grading index (p)

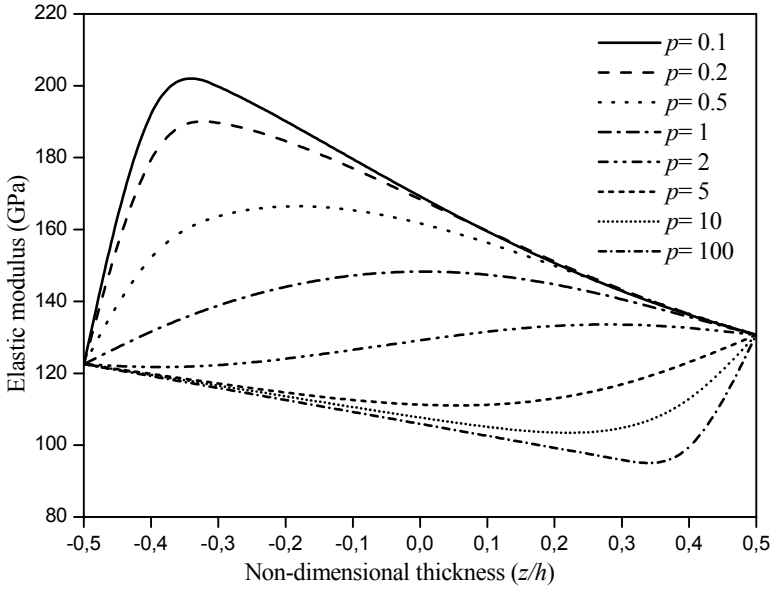

Fig. 4 Variation of elastic modulus versus non-dimensional thickness of FG plate in nonlinear temperature field and different values of grading index (p)

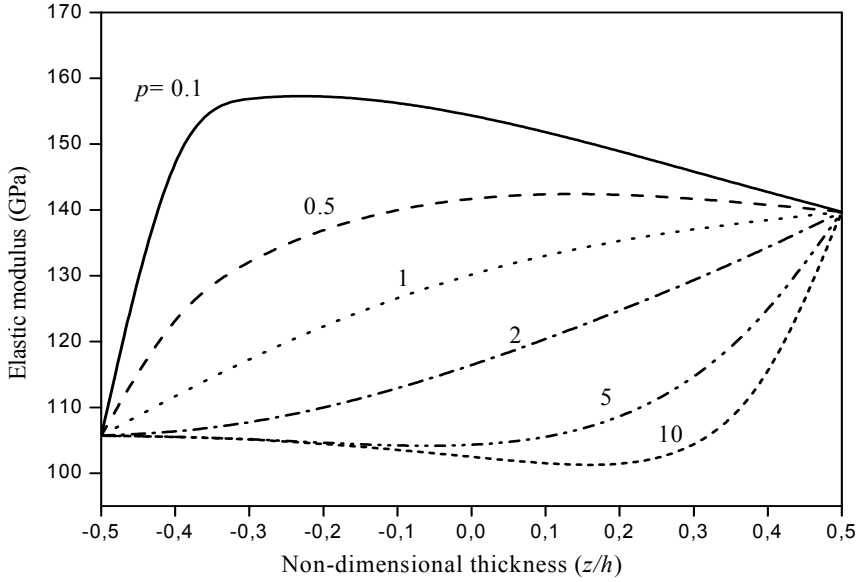

Fig. 5 Variation of elastic modulus versus non-dimensional thickness of FG plate in sinusoidal temperature field and different values of grading index (p)

Figs. 2 and 3 show that Young's modulus is similar for conditions with room temperature and linear temperature variation, but the graphs move to smaller values with the linear temperature case. It is seen clearly, that with increasing the power law index, the Young's modulus decreases. In addition, it can be observed from Figs. 2 to 6 that the behavior of Young's modulus in nonlinear

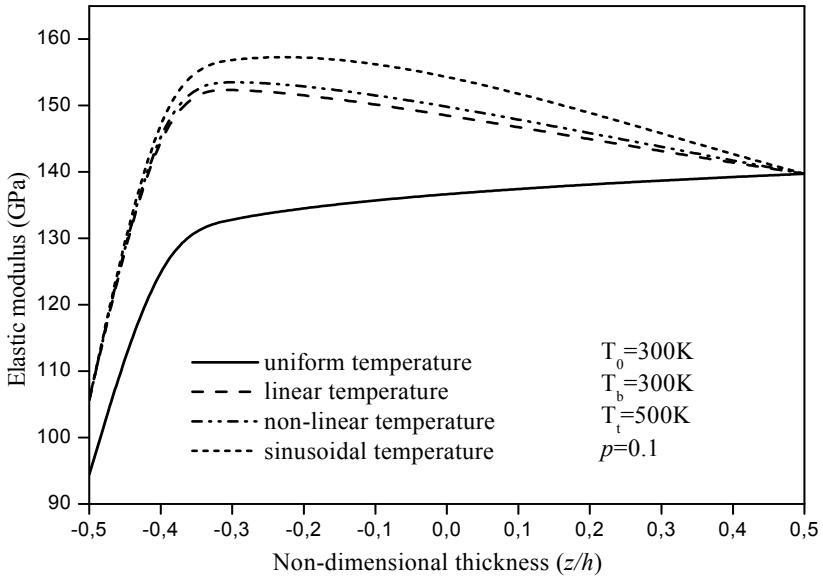

Fig. 6 Variation of elastic modulus versus non-dimensional thickness of FG plate in uniform, linear, nonlinear and sinusoidal temperature field

and sinusoidal thermal loads is completely different from that in room and linear temperature cases. Thus, it can be concluded that the environmental conditions type has a considerable effect on Young's modulus. A comparison study on Young's modulus is carried out for uniform, linear, nonlinear and sinusoidal thermal conditions in Fig. 6.

4.2 Validation of the results

In this section, various numerical results for temperature-dependent FG plates computed using the present theories having four unknowns are compared to those of other higher-order shear deformation theories [15, 23] with more unknowns. The nondimensional frequency parameter is taken as, where and is at (Shahrjerdi *et al*. 2011, Huang and Shen 2004).

Example 1

In the first example, a FG ZrO_2/Ti–6Al–4V plate is considered and the dimensionless fundamental frequencies are tabulated in Table 3. As is described in references (Shahrjerdi *et al*. 2011, Huang and Shen 2004), the top surface is ceramic-rich and the bottom surface is metal-rich. Verification is carried out by assuming the values of different quantities in the ceramic and metal as: h = 0.0025 m, $a = b$ = 0.2 m, v = 0.3, ρ_c = 3000 km/m^3, k_c = 1.80 W/mK, ρ_m = 4429 kg/m^3, k_m 7.82 W/mK.

An identical value of Poisson's ratio v is assumed for both ceramic and metal. However, Young's modulus and thermal expansion coefficient of these materials are considered to be temperature-dependent (Shahrjerdi *et al*. 2011, Huang and Shen 2004). It can be seen from Table 3 that the results computed using various efficient higher-order shear deformation theories (TPT, SPT, HPT and EPT) are in a good agreement with other results from Refs (Shahrjerdi *et al*. 2011, Huang and Shen 2004) especially obtained by Huang and Shen (2004) and these for all values of

Table 3 Non-dimensional natural frequency parameter of simply supported (ZrO_2/Ti-6Al-4V) FG plate in thermal environments

Mode (1,1) Natural frequency of FGP (ZrO_2 and Ti-6Al-4V)		T_b = 300 (K)				
		T_t = 300 (K)	T_t = 400 (K)		T_t = 600 (K)	
			Temperature-dependent	Temperature-independent	Temperature-dependent	Temperature-independent
ZrO_2	SSDT[a]	8.333	7.614	7.892	5.469	6.924
	TSDT[b]	8.273	7.868	8.122	6.685	7.686
	TPT	8.278	7.807	8.130	6.533	7.826
	SPT	8.278	7.808	8.131	6.534	7.826
	HPT	8.278	7.808	8.131	6.534	7.826
	EPT	8.280	7.809	8.132	6.536	7.828
p = 0.5	SSDT[a]	7.156	6.651	6.844	5.255	6.175
	TSDT[b]	7.139	6.876	7.154	6.123	6.776
	TPT	7.111	6.781	7.005	5.931	6.789
	SPT	7.112	6.782	7.006	5.931	6.789
	HPT	7.112	6.782	7.006	5.931	6.789
	EPT	7.113	6.783	7.001	5.993	6.772
p = 1	SSDT[a]	6 .700	6.281	6.446	5.167	5.904
	TSDT[b]	6.657	6.437	6.592	5.819	6.362
	TPT	6.657	6.375	6.565	5.664	6.378
	SPT	6.657	6.375	6.565	5.665	6.378
	HPT	6.657	6.375	6.565	5.665	6.378
	EPT	6.658	6.376	6.556	5.668	6.350
p = 2	SSDT[a]	6.333	5.992	6.132	5.139	5.711
	TSDT[b]	6.286	6.101	6.238	5.612	6.056
	TPT	6.287	6.047	6.208	5.467	6.049
	SPT	6.287	6.047	6.208	5.467	6.049
	HPT	6.287	6.047	6.208	5.467	6.049
	EPT	6.288	6.049	6.194	5.469	6.003
Ti-6Al-4V	SSDT[a]	5.439	5.103	5.333	4.836	5.115
	TSDT[b]	5.400	5.322	5.389	5.118	5.284
	TPT	5.403	5.303	5.361	5.132	5.275
	SPT	5.403	5.303	5.361	5.132	5.275
	HPT	5.403	5.303	5.361	5.132	5.275
	EPT	5.404	5.304	5.300	5.133	5.091

[a] Shahrjerdi *et al*. (2011)
[b] Huang and Shen (2004)

power law index p, either for the case of temperature-dependent and temperature-independent FG plates (FGP).

Example 2

In the next example, a FG Si_3N_4/SUS304 plate is analyzed. For this materials, the Poisson's ratio is taken $v = 0.28$. The dimensionless fundamental frequencies obtained by all present theories are compared with the previously published results of Shahrjerdi *et al*. (2011) and Huang and Shen (2004) in Table 4 for different values of power law index p. It can be seen that the fundamental frequency values computed from all proposed theories are in a good agreement with those given by Refs (Shahrjerdi *et al*. 2011, Huang and Shen 2004) especially obtained by Huang and Shen (2004).

Example 3

In this example, a ZrO_2/Ti–6Al–4V and Si_3N_4/SUS304 plates are considered and the obtained

Table 4 Non-dimensional natural frequency parameter of simply supported (Si_3N_4/SUS304) FG plate in thermal environments

Mode (1,1) Natural frequency of FGP (Si_3N_4 and SUS304)		$T_b = 300$ (K)				
			$T_t = 400$ (K)		$T_t = 600$ (K)	
		$T_t = 300$ (K)	Temperature-dependent	Temperature-independent	Temperature-dependent	Temperature-independent
Si_3N_4	SSDT[(a)]	12.506	12.175	12.248	11.461	11.716
	TSDT[(b)]	12.495	12.397	12 .382	11.984	12.213
	TPT	12.507	12.307	12.376	11.886	12.113
	SPT	12.507	12.307	12.378	11.887	12.114
	HPT	12.507	12.307	12.378	11.886	12.114
	EPT	12.509	12.309	12.380	11.889	12.116
$p = 0.5$	SSDT[(a)]	8.652	8.361	8.405	7.708	7.887
	TSDT[(b)]	8.675	8.615	8.641	8.269	8.425
	TPT	8.609	8.453	8.498	8.117	8.272
	SPT	8.609	8.453	8.499	8.118	8.273
	HPT	8.609	8.453	8.499	8.118	8.273
	EPT	8.611	8.455	8.500	8.120	8.274
$p = 1$	SSDT[(a)]	7.584	7.306	7.342	6.674	6.834
	TSDT[(b)]	7.555	7.474	7.514	7.171	7.305
	TPT	7.544	7.399	7.437	7.082	7.217
	SPT	7.544	7.399	7.437	7.082	7.218
	HPT	7.544	7.399	7.437	7.082	7.218
	EPT	7.546	7.401	7.439	7.083	7.219

Table 4 Continued

Mode (1,1) Natural frequency of FGP (Si_3N_4 and SUS304)		T_b = 300 (K)				
			T_t = 400 (K)		T_t = 600 (K)	
		T_t = 300 (K)	Temperature-dependent	Temperature-independent	Temperature-dependent	Temperature-independent
p = 2	SSDT[(a)]	6.811	6.545	6.575	5.929	6.077
	TSDT[(b)]	6.777	6.693	6.728	6.398	6.523
	TPT	6.771	6.631	6.664	6.323	6.447
	SPT	6.770	6.631	6.665	6.323	6.447
	HPT	6.770	6.631	6.665	6.323	6.447
	EPT	6.772	6.633	6.665	6.324	6.448
SUS304	SSDT[(a)]	5.410	5.161	5.178	4.526	4.682
	TSDT[(b)]	5.405	5.311	5.335	4.971	5.104
	TPT	5.410	5.272	5.295	4.922	5.055
	SPT	5.410	5.278	5.300	4.945	5.071
	HPT	5.410	5.278	5.299	4.945	5.071
	EPT	5.411	5.279	5.301	4.946	5.073

[(a)] Shahrjerdi *et al*. (2011)
[(b)] Huang and Shen (2004)

results are compared to those of Shahrjerdi *et al*. (2011) and Huang and Shen (2004) as shown in Tables 5 and 6, respectively. It can be seen that the computed results are in good agreement with the previously published results (Shahrjerdi *et al*. 2011, Huang and Shen 2004) and these for different considered shape mode.

Table 5 Non-dimensional frequency parameter of simply supported (ZrO_2/Ti-6Al-4V) FG plate in thermal environments (p = 2)

Mode numbers of FGP (ZrO_2 and Ti-6Al-4V)		T_b = 300 (K)				
			T_t = 300 (K)		T_t = 300 (K)	
		T_t = 300 (K)	Temperature-dependent	Temperature-independent	Temperature-dependent	Temperature-independent
(1,1)	SSDT[(a)]	6.333	5.992	6.132	5.139	5.711
	TSDT[(b)]	6.286	6.101	6.238	5.612	6.056
	TPT	6.287	6.047	6.208	5.467	6.049
	SPT	6.287	6.047	6.208	5.467	6.049
	HPT	6.287	6.047	6.208	5.467	6.049
	EPT	6.288	6.049	6.194	5.469	6.003

Table 5 Continued

Mode numbers of FGP (ZrO_2 and Ti-6Al-4V)		T_b = 300 (K)				
			T_t = 300 (K)		T_t = 300 (K)	
		T_t = 300 (K)	Temperature-dependent	Temperature-independent	Temperature-dependent	Temperature-independent
(1,2)	SSDT[(a)]	14.896	14.383	14.684	13.260	14.253
	TSDT[(b)]	14.625	14.372	14.655	13.611	14.474
	TPT	14.665	14.265	14.581	13.416	14.412
	SPT	14.666	14.267	14.583	13.416	14.414
	HPT	14.665	14.265	14.581	13.413	14.413
	EPT	14.672	14.273	14.589	13.421	14.420
(2,2)	SSDT[(a)]	22.608	21.942	22.386	20.557	21.935
	TSDT[(b)]	21.978	21.653	22.078	20.652	21.896
	TPT	22.123	21.584	22.034	20.489	21.855
	SPT	22.127	21.589	22.038	20.494	21.860
	HPT	22.123	21.584	22.034	20.489	21.855
	EPT	22.140	21.602	22.052	20.507	21.873
(1,3)	SSDT[(a)]	27.392	26.630	27.163	25.077	26.700
	TSDT[(b)]	26.454	26.113	26.605	24.961	26.435
	TPT	26.704	26.081	26.612	24.837	26.427
	SPT	26.711	26.089	26.619	24.845	26.435
	HPT	26.704	26.081	26.612	24.837	26.427
	EPT	26.731	26.108	26.639	24.865	26.454
(2,3)	SSDT[(a)]	34.106	33.211	33.867	31.425	33.384
	TSDT[(b)]	32.659	32.239	32.840	30.904	32.664
	TPT	33.109	32.371	33.013	30.920	32.819
	SPT	33.121	32.384	33.025	30.933	32.831
	HPT	33.109	32.370	33.013	30.919	32.819
	EPT	33.151	32.413	33.055	30.964	32.862

[(a)] Shahrjerdi *et al*. (2011)
[(b)] Huang and Shen (2004)

Example 4

Table 7 shows the natural frequencies in Si3N4/SUS304 for large value of volume fraction index (p) and different values of thermal loads. Again, a good agreement between the present results and those of Shahrjerdi *et al*. (2011) is observed. The little difference observed in the results between the present theories (TPT, SPT, HPT and EPT) and the second-order shear deformation theory (SSDT) of Shahrjerdi *et al*. (2011) is due to the displacement fields assumed

Table 6 Non-dimensional frequency parameter of simply supported (Si_3N_4/SUS304) FG plate in thermal environments ($p = 2$)

Mode numbers of FGP (Si_3N_4/SUS304)		$T_b = 300$ (K)				
		$T_t = 300$ (K)	$T_t = 300$ (K)		$T_t = 300$ (K)	
			Temperature-dependent	Temperature-independent	Temperature-dependent	Temperature-independent
(1,1)	SSDT[a]	6.811	6.445	6.575	5.929	6.077
	TSDT[b]	6.777	6.693	6.728	6.398	6.523
	TPT	6.770	6.631	6.664	6.323	6.447
	SPT	6.770	6.631	6.664	6.323	6.447
	HPT	6.770	6.631	6.664	6.323	6.447
	EPT	6.770	6.631	6.665	6.325	6.448
(1,2)	SSDT[a]	16.017	15.708	15.769	15.002	15.262
	TSDT[b]	15.809	15.762	15.836	15.384	15.632
	TPT	15.812	15.628	15.699	15.229	15.472
	SPT	15.814	15.631	15.702	15.231	15.474
	HPT	15.812	15.628	15.699	15.229	15.472
	EPT	15.820	15.636	15.707	15.237	15.480
(2,2)	SSDT[a]	24.307	23.958	24.047	23.154	23.517
	TSDT[b]	23.806	23.786	23.893	23.327	23.685
	TPT	23.874	23.652	23.755	23.167	23.517
	SPT	23.879	23.657	23.760	23.173	23.522
	HPT	23.874	23.652	23.755	23.167	23.516
	EPT	23.893	23.671	23.774	23.187	23.536
(1,3)	SSDT[a]	29.446	29.071	29.177	28.204	28.632
	TSDT[b]	28.687	28.686	28.816	28.185	28.609
	TPT	28.831	28.586	28.709	28.049	28.463
	SPT	28.839	28.594	28.717	28.057	28.471
	HPT	28.831	28.586	28.709	28.049	28.462
	EPT	28.860	28.614	28.738	28.078	28.491
(2,3)	SSDT[a]	36.657	36.247	36.376	35.290	35.809
	TSDT[b]	35.466	35.491	35.648	34.918	35.436
	TPT	35.768	35.489	35.640	34.879	35.383
	SPT	35.782	35.503	35.654	34.893	35.397
	HPT	35.768	35.489	35.640	34.878	35.383
	EPT	35.814	35.535	35.686	34.925	35.429

[a] Shahrjerdi *et al*. (2011)
[b] Huang and Shen (2004)

by these theories. It should be noted that the present theories require only four unknowns as against seven in the case of SSDT (Shahrjerdi *et al*. 2011). It can be concluded that the present theory is not only accurate but also efficient in predicting the vibration response of FG plates.

Table 7 Non-dimensional natural frequency of temperature dependent (Si_3N_4/SUS304) FG plate for different volume fraction index p in thermal environments, Mode (1, 1)

Thermal loads $T_0 = 300$ (K), $b = a = 0.2$, $h = 0.025$		$T_b = 300$ (K) $T_t = 300$ (K)	$T_b = 300$ (K) $T_t = 400$ (K)	$T_b = 300$ (K) $T_t = 600$ (K)
Si_3N_4	SSDT[(a)]	12.506	12.175	11.461
	TPT	12.506	12.306	11.886
	SPT	12.507	12.307	11.887
	HPT	12.507	12.307	11.887
	EPT	12.509	12.309	11.889
$p = 0.5$	SSDT[(a)]	6.200	5.936	5.328
	TPT	6.151	6.014	5.703
	SPT	6.151	6.015	5.704
	HPT	6.151	6.015	5.704
	EPT	6.152	6.016	5.705
$p = 10$	SSDT[(a)]	5.907	5.645	5.031
	TPT	5.862	5.725	5.405
	SPT	5.862	5.725	5.405
	HPT	5.862	5.725	5.405
	EPT	5.863	5.723	5.407
$p = 20$	SSDT[(a)]	5.711	5.450	4.825
	TPT	5.671	5.532	5.203
	SPT	5.671	5.532	5.203
	HPT	5.671	5.532	5.203
	EPT	5.672	5.534	5.204
$p = 40$	SSDT[(a)]	5.591	5.329	4.694
	TPT	5.552	5.414	5.076
	SPT	5.552	5.414	5.076
	HPT	5.552	5.414	5.076
	EPT	5.553	5.416	5.077
SUS304	SSDT[(a)]	5.410	5.161	4.526
	TPT	5.410	5.273	4.926
	SPT	5.410	5.273	4.926
	HPT	5.410	5.273	4.926
	EPT	5.411	5.274	4.927

[(a)] Shahrjerdi *et al*. (2011)

4.3 Results of present study

The effects different parameters such as the power law index, the mode numbers, plate geometry, and temperature fields on the frequency of FG plates are investigated here. All predicted results are carried out using TPT.

The non-dimensional frequencies values are listed in Tables 8 and 9 for FG ZrO_2/Ti–6Al–4V and Si_3N_4/SUS304 plates, respectively. The non-dimensional natural frequency parameter is defined as $\overline{\omega} = \omega(a^2/h)\left[\rho_b(1-\nu^2)/E_b\right]^{1/2}$, where E_b and ρ_b are at T_0 = 300 (K) (Shahrjerdi *et al*. 2011). The effect of power law index p on the frequencies can be seen by considering the same value of thermal load and shape mode. The result for FG plates is in between those for pure material plates, because Young's modulus increases from pure metal to pure ceramic. The frequencies are decreased by increasing the temperature difference between top and bottom surfaces for the same value of power law index and shape mode that represent the effects of thermal loads. The comparison between temperature-dependent and independent FG plates in Tables 8 and 9 reveals the smaller frequencies in temperature-dependent FG plates, which proves the accuracy and effectiveness of temperature-dependent material properties.

The variation of the first four frequencies as a function of uniform, linear, nonlinear and sinusoidal temperature fields in simply supported FG plate is plotted in Figs. 7-10. The combination of ZrO_2/Ti-6Al-4V (Table 2) is assumed with material and geometric parameters of

Table 8 Non-dimensional natural frequency parameter of simply supported (ZrO_2/Ti-6Al-4V) FG plate in thermal environments and for different modes of vibration

Mode numbers of FGP (ZrO_2 and Ti-6Al-4V)		T_b = 300 (K)				
			T_t = 400 (K)		T_t = 600 (K)	
		T_t = 300 (K)	Temperature-dependent	Temperature-independent	Temperature-dependent	Temperature-independent
ZrO_2	(1,1)	8.278	7.808	8.131	6.534	7.826
	(1,2)	19.344	18.577	19.054	16.842	18.867
	(2,2)	29.217	28.185	28.911	26.002	28.714
	(1,3)	35.292	34.095	34.975	31.632	34.472
	(2,3)	43.794	42.368	43.462	39.509	43.250
p = 0.5	(1,1)	7.112	6.782	7.006	5.931	6.789
	(1,2)	16.631	16.093	16.518	14.902	16.367
	(2,2)	25.138	24.415	25.019	22.908	24.779
	(1,3)	30.376	29.540	30.159	27.837	30.006
	(2,3)	37.713	36.720	37.486	34.744	37.326
p = 1	(1,1)	6.657	6.375	6.565	5.664	6.378
	(1,2)	15.558	15.095	15.392	14.084	15.264
	(2,2)	21.596	22.882	23.329	21.596	23.194
	(1,3)	26.221	27.676	28.213	26.221	28.074
	(2,3)	35.243	34.389	35.052	32.698	34.907

Table 8 Continued

Mode numbers of FGP (ZrO_2 and Ti-6Al-4V)		T_b = 300 (K)				
			T_t = 400 (K)		T_t = 600 (K)	
		T_t = 300 (K)	Temperature-dependent	Temperature-independent	Temperature-dependent	Temperature-independent
p = 2	(1,1)	6.287	6.047	6.208	5.467	6.049
	(1,2)	14.666	14.267	14.583	13.416	14.414
	(2,2)	22.127	21.589	22.038	20.494	21.860
	(1,3)	26.711	26.089	26.619	24.845	26.435
	(2,3)	33.121	32.384	33.025	30.933	32.831
Ti-6Al-4V	(1,1)	5.403	5.303	5.361	5.132	5.275
	(1,2)	12.625	12.440	12.580	12.096	12.489
	(2,2)	19.069	18.811	19.022	18.314	18.926
	(1,3)	23.035	22.730	22.985	22.142	22.886
	(2,3)	28.584	28.217	28.532	27.499	28.428

Table 9 Non-dimensional natural frequency parameter of simply supported (Si_3N_4/ SUS304) FG plate in thermal environments and for different modes of vibration

Mode numbers of FGP (Si_3N_4 and SUS304)		T_b = 300 (K)				
			T_t = 300 (K)		T_t = 300 (K)	
		T_t = 300 (K)	Temperature-dependent	Temperature-independent	Temperature-dependent	Temperature-independent
Si_3N_4	(1,1)	12.507	12.307	12.377	11.887	12.114
	(1,2)	29.260	28.964	29.121	28.371	28.843
	(2,2)	44.236	43.853	44.090	43.103	43.796
	(1,3)	53.460	53.024	53.309	52.176	53.005
	(2,3)	66.382	65.310	66.240	64.886	65.906
p = 0.5	(1,1)	8.609	8.453	8.498	8.118	8.272
	(1,2)	20.137	19.921	20.020	19.473	19.784
	(2,2)	30.441	30.172	30.318	29.621	30.070
	(1,3)	36.788	36.485	36.661	35.871	36.405
	(2,3)	45.680	45.331	45.547	44.627	45.281
p = 1	(1,1)	7.544	7.399	7.437	7.082	7.217
	(1,2)	17.641	17.444	17.528	17.029	17.298
	(2,2)	26.661	26.420	26.542	25.913	26.301
	(1,3)	32.215	31.946	32.092	31.384	31.970
	(2,3)	39.995	39.688	39.867	39.046	39.608

Table 9 Continued

Mode numbers of FGP (Si_3N_4 and SUS304)		T_b = 300 (K)				
			T_t = 300 (K)		T_t = 300 (K)	
		T_t = 300 (K)	Temperature-dependent	Temperature-independent	Temperature-dependent	Temperature-independent
p = 2	(1,1)	6.770	6.631	6.664	6.323	6.447
	(1,2)	15.814	15.631	15.702	15.231	15.474
	(2,2)	23.879	23.657	23.760	23.173	23.522
	(1,3)	28.839	28.594	28.717	28.057	28.471
	(2,3)	35.782	35.503	35.654	34.893	35.397
SUS304	(1,1)	5.410	5.278	5.300	4.945	5.071
	(1,2)	12.657	12.495	12.539	12.054	12.301
	(2,2)	19.135	18.947	19.012	18.407	18.760
	(1,3)	23.126	22.920	22.908	22.320	22.738
	(2,3)	28.715	28.487	28.581	27.803	28.310

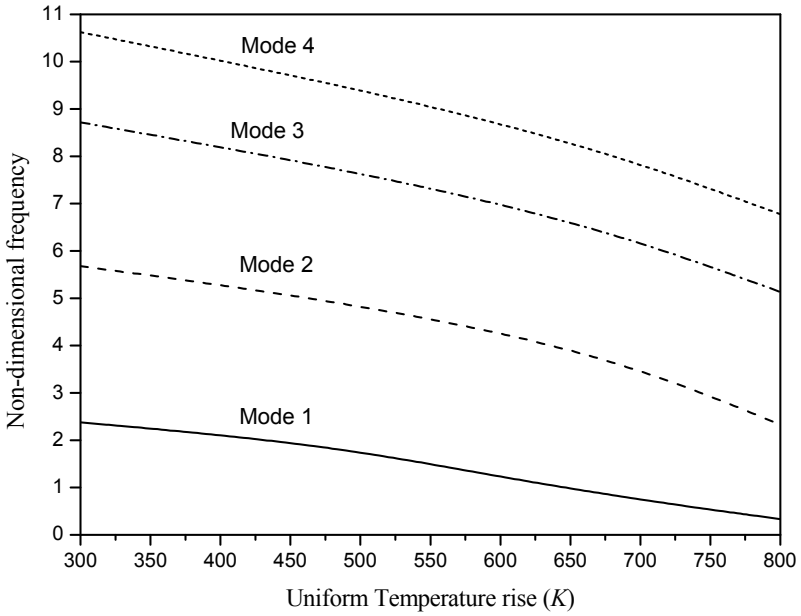

Fig. 7 First four Non-dimensional frequency parameters versus uniform temperature field for simply supported (ZrO_2/Ti-6Al-4V) FGP when $a / h = 10$ and $a = 0.2$, $p = 1$

$p = 1$, $a = b = 0.2$ and $a / h = 10$. The non-dimensional natural frequency parameter is defined as $\overline{\omega} = \omega(b^2 / \pi^2)\left[I_0 / D_0\right]^{1/2}$, where $I_0 = \rho h$ and $D_0 = Eh^3 / 12(1 - v^2)$ and it is noted that ρ, v and E are chosen to be the values of Ti-6Al-4V evaluated at the room temperature. As expected, the frequencies are reduced with increasing temperature and this is due to the decrease of Young's

modulus with rising temperatures. It can be seen that the decreasing slope of frequencies in lower modes is smaller than those in higher modes. At the same temperature, we note that the difference between two consecutive lower modes is greater than that in two consecutive higher modes.

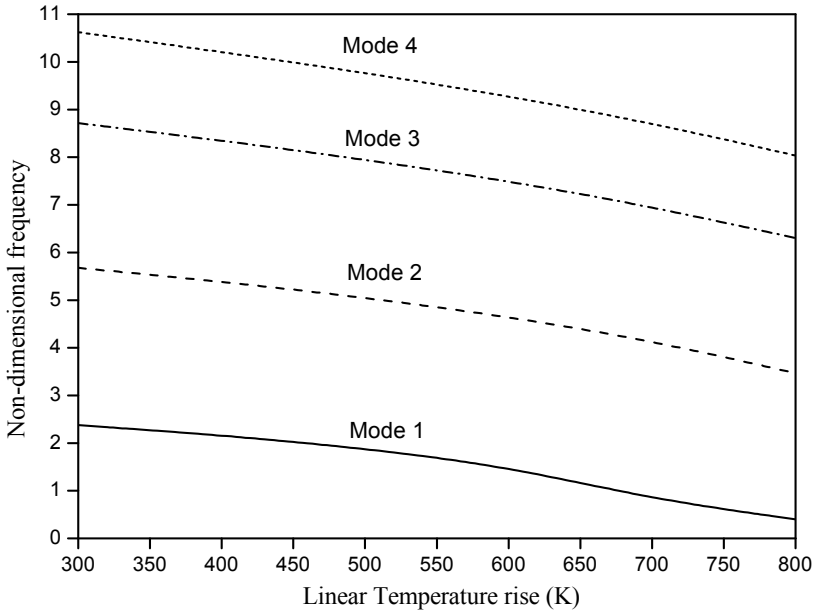

Fig. 8 First four Non-dimensional frequency parameters versus linear temperature field for simply supported (ZrO_2/Ti-6Al-4V) FGP when a / h = 10 and a = 0.2, p = 1

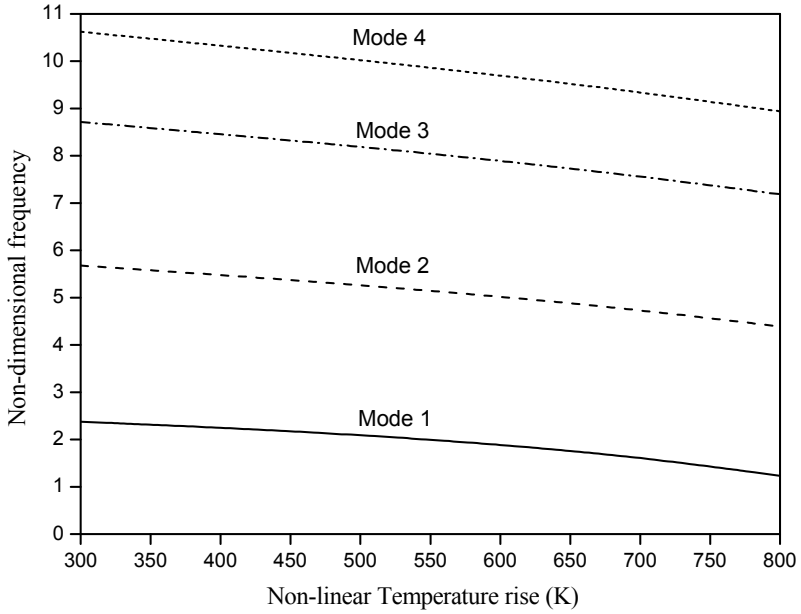

Fig. 9 First four Non-dimensional frequency parameters versus non-linear temperature field for simply supported (ZrO_2/Ti-6Al-4V) FGP when a / h = 10 and a = 0.2, p = 1

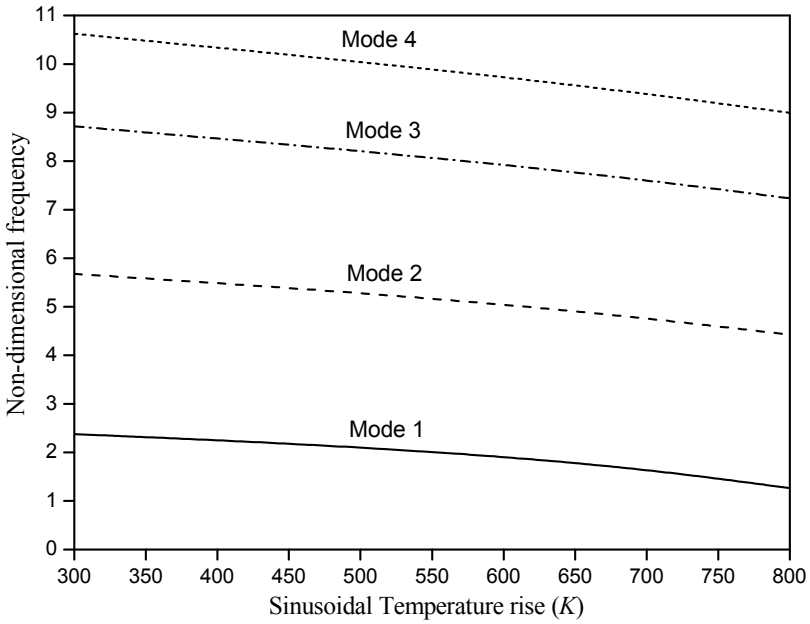

Fig. 10 First four Non-dimensional frequency parameters versus sinusoidal temperature field for simply supported (ZrO_2/Ti-6Al-4V) FGP when $a / h = 10$ and $a = 0.2$, $p = 1$

5. Conclusions

In this research study, temperature-dependent free vibration of FG plates subjected to uniform, linear, nonlinear, and sinusoidal temperature fields is presented by using various efficient higher-order shear deformation theories. The main advantage of the proposed theories over the existing higher-order shear deformation theories is that the present ones involve fewer variables as well as equations of motion. The computational cost can therefore be reduced. Material properties of FG plates are assumed to be temperature-dependent and graded through the thickness according to a power-law distribution in terms of volume fractions of constituents. Numerical results show that all proposed theories give results close to each other, and their solutions are in good agreement with those of existing higher-order shear deformation theories such as the second-order shear deformation theory (SSDT) and third-order shear deformation theory. The formulation lends itself particularly well to nonlinear vibration of FG structures (Yaghoobi and Torabi 2013a, b), which will be considered in the near future.

References

Ait Atmane Meziane, H., Tounsi, A. and Adda Bedia, E.A. (2010), "Free vibration analysis of functionally graded plates resting on Winkler-Pasternak elastic foundations using a new shear deformation theory", *International Journal of Mechanics and Materials in Design*, **6**(2), 113-121.

Ait Atmane Meziane, M., Abdelaziz, H.H. and Tounsi, A. (2014), "An efficient and simple refined theory for buckling and free vibration of exponentially graded sandwich plates under various boundary conditions", *J. Sandwich Struct. Mater.*, **16**(3), 293-318.

Akavci, S. (2010), "Two new hyperbolic shear displacement models for orthotropic laminated composite plates", *Mech. Compos. Mater.*, **46**(2), 215-226.
Bouazza, M., Tounsi, A., Adda Bedia, E.A. and Megueni, A. (2009), "Buckling analysis of functionally graded plates with simply supported edges", *Leonardo Journal of Sciences*, **15**(8), 2-32.
Bouderba, B., Houari, M.S.A. and Tounsi, A. (2013), "Thermomechanical bending response of FGM thick plates resting on Winkler-Pasternak elastic foundations", *Steel Compos. Struct., Int. J.*, **14**(1), 85-104.
Bourada, M., Tounsi, A., Houari, M.S.A. and Adda Bedia, E.A. (2012), "A new four-variable refined plate theory for thermal buckling analysis of functionally graded sandwich plates", *J. Sandwich Struct. Mater.*, **14**(1), 5-33.
Chi, S. and Chung, Y. (2006a), "Mechanical behavior of functionally graded material plates under transverse load. Part I: Analysis", *Int. J. Sol. Struct.*, **43**(13), 3657-3674.
Chi, S. and Chung, Y. (2006b), "Mechanical behavior of functionally graded material plates under transverse load. Part II: Numerical results", *Int. J. Sol. Struct.*, **43**(13), 3675-3691.
Grover, N., Maiti, D.K. and Singh, B.N. (2013), "A new inverse hyperbolic shear deformation theory for static and buckling analysis of laminated composite and sandwich plates", *Compos. Struct.*, **95**, 667-675.
Fekrar, A., El Meiche, N., Bessaim, A., Tounsi, A. and Adda Bedia, E.A. (2012), "Buckling analysis of functionally graded hybrid composite plates using a new four variable refined plate theory", *Steel Compos. Struct., Int. J.*, **13**(1), 91-107.
Huang, X. and Shen, H. (2004), "Nonlinear vibration and dynamic response of functionally graded plates in thermal environments", *Int. J. Solid. Struct.*, **41**(9-10), 2403-2427.
Karama, M., Afaq, K.S. and Mistou, S. (2003), "Mechanical behaviour of laminated composite beam by the new multi-layered laminated composite structures model with transverse shear stress continuity", *Int. J. Solids Struct.*, **40**(6), 1525-1546.
Kettaf, F.Z., Houari, M.S.A., Benguediab, M. and Tounsi, A. (2013), "Thermal buckling of functionally graded sandwich plates using a new hyperbolic shear displacement model", *Steel Compos. Struct., Int. J.*, **15**(4), 399-423.
Kim, Y. (2005), "Temperature dependent vibration analysis of functionally graded rectangular plates", *J. Sound Vib.*, **284**(3-5), 531-549.
Li, Q., Iu, V. and Kou, K. (2009), "Three-dimensional vibration analysis of functionally graded material plates in thermal environment", *J. Sound Vib.*, **324**(3-5), 733-750.
Mantari, J.L., Oktem, A.S. and Guedes Soares, C. (2012), "A new trigonometric shear deformation theory for isotropic, laminated composite and sandwich plates", *Int. J. Solids Struct.*, **49**(1), 43-53.
Mindlin, R.D. (1951), "Influence of rotatory inertia and shear on flexural motions of isotropic, elastic plates", *J. Appl.Mech.*, **18**(1), 31-38.
Pradyumna, S. and Bandyopadhyay, J.N. (2008), "Free vibration analysis of functionally graded curved panels using a higher-order finite element formulation", *J. Sound Vib.*, **318**(1-2), 176-192.
Reddy, J.N. (1984), "A simple higher-order theory for laminated composite plates", *J. Appl. Mech.*, **51**(4), 745-752.
Reddy, J.N. (2000), "Analysis of functionally graded plates", *Int. J. Numer. Method. Eng.*, **47**(1-3), 663-684.
Reddy, J.N. (2004), *Mechanics of Laminated Composite Plates and Shells*, CRC Press.
Reissner, E. (1945), "The effect of transverse shear deformation on the bending of elastic plates", *J. Appl. Mech.*, **12**(2), 69-72.
Ren, J.G. (1986), "A new theory of laminated plate", *Compos. Sci. Technol.*, **26**(3), 225-239.
Shahrjerdi, A., Mustapha, F., Bayat, M. and Majid, D.L.A. (2011), "Free vibration analysis of solar functionally graded plates with temperature-dependent material properties using second order shear deformation theory", *J. Mech. Sci. Techol.*, **25**(9), 2195-2209.
Soldatos, K.P. (1992), "A transverse shear deformation theory for homogeneous monoclinic plates", *Acta Mech.*, **94**(3), 195-220.
Touratier, M. (1991), "An efficient standard plate theory", *Int. J. Eng. Sci.*, **29**(8), 901-916.
Xiang, S., Wang, K.M., Ai, Y.T., Sha, Y.D. and Shi, H. (2009), "Analysis of isotropic, sandwich and

laminated plates by a meshless method and various shear deformation theories", *Compos. Struct.*, **91**(1), 31-37.

Yaghoobi, H. and Torabi, M. (2013a), "Post-buckling and nonlinear free vibration analysis of geometrically imperfect functionally graded beams resting on nonlinear elastic foundation", *Appl. Math. Model.*, **37**(18-19), 8324-8340.

Yaghoobi, H. and Torabi, M., (2013b), "An analytical approach to large amplitude vibration and post-buckling of functionally graded beams rest on non-linear elastic foundation", *J. Theor. Appl. Mech.*, **51**(1), 39-52.

Yaghoobi, H. and Yaghoobi, P. (2013), "Buckling analysis of sandwich plates with FGM face sheets resting on elastic foundation with various boundary conditions: An analytical approach", *Meccanica*, **48**(8), 2019-2035.

CC